Tutorial

John R. Rogers*

The importance of induced aberrations in the correction of secondary color

Abstract: Much publicity has been given to the art and science of choosing glass types for the reduction of secondary color, particularly for systems (such as achromats) in which all the elements are in contact. Although it has long been recognized that airspaces between elements can influence chromatic aberration and can even be used to reduce or correct secondary color, comparatively, little emphasis has been placed on this in the published literature. This tutorial is intended to call attention to the induced component of secondary color and suggests methods for improving color correction.

Keywords: chromatic aberration; secondary color.

OCIS codes: 220.0220; 080.0080; 080.3620; 080.2740.

*Corresponding author: **John R. Rogers**, Synopsys, Inc., OSG 3280 E. Foothill Blvd., Pasadena, CA 91107, USA, e-mail: jrogers@synopsys.com

1 Introduction

Over the years, a great deal has been published concerning the selection of optical glasses for the purpose of correcting chromatic aberration, with emphasis on the correction of secondary and higher-order color in thin elements [1–14]. Although glass selection is important for the direct control of chromatic aberration, it is equally important to recognize the role of induced (also known as extrinsic) aberration in the correction of chromatic aberration. Although this point was clearly understood by the authors referenced, the strong emphasis on glass selection in the publications focuses the attention on the properties of the glasses, themselves, and diverts attention away from the effect that large airspaces have on the state of color correction. This paper is intended as a tutorial to encourage consideration of the induced color aberrations.

Before going further, it is useful to point out that regardless of the formalism used to select glasses, one finds that

from the standpoint of color correction, the most desirable glasses are those of the FK, KZFS, and LASF series from Schott and equivalent glasses from other manufacturers. If more than two glasses can be used for achromatization, then the high-index SF glasses are also useful. Unfortunately, these glass types have many disadvantages. For the sake of simplicity, all glass types mentioned in this tutorial are from Schott [15]; similar glass types are available from other manufacturers. The FK glasses are expensive and have a sufficiently high coefficient of thermal expansion (CTE) that they break when exposed to a thermal shock. This property makes the glass not only expensive to purchase but also expensive to work. (Many fabrication shops simply refuse to work with such glasses.) Furthermore, the FK glasses, in many cases, cannot be used in cemented doublets because the CTE mismatch between the crown and flint elements would cause delamination of the cement layer over a reasonable storage temperature range. The KZFS glasses have relatively low CTE values and, as singlets, are not susceptible to thermal shock breakage; however, cementing them to high-expansion FK glasses can be problematic even over modest temperature ranges. The KZFS glasses are expensive. (Of the glasses for which Schott lists prices, KZFSN11 is the most expensive, being 30 times more expensive than BK7.) The LASF glasses are also expensive and suffer more bulk absorption than the FK and KZFS types. The SF glasses (particularly the lead-free NSF types) tend to have poor transmission in the blue. In almost all real designs, the use of these glasses is restricted in some way by these undesirable properties of these otherwise advantageous glasses. For all of these reasons, it is important to understand the origin of the induced chromatic aberration terms (and how to manipulate them) without resorting to more exotic glass types.

2 The Schuppmann one-glass achromat

We begin by exploring the properties of an all-diffractive version of the well-known Schuppmann one-glass

achromat [16]. The diffractive version of this system, comprising elements that are separated but individually infinitely thin, is a perfect system to study because the so-called 'thin lens equations' may be applied without concern that they are inaccurate because of the finite thickness of the parts or because (in lens elements) there are two surfaces to consider rather than one. (In the following, we will consider the holograms to be thin Fresnel zone plates so that the substrates can be ignored.)

Since its original description, the Schuppmann system has been discovered by several authors [17–19] for diffractive applications, and it is important in this context to understand the analogy of diffractive systems to refractive systems. For a glass element, and for the d, F, and C spectral lines commonly used in the visible spectrum, the Abbe value is defined as:

$$v = \frac{n_d - 1}{n_F - n_C} \tag{1}$$

The physical significance of the Abbe value is that it is proportional to $\phi/\Delta_{FC}(\phi)$ where ϕ is the power (at the d wavelength) of an element made of this glass, and $\Delta_{FC}(\phi)$ represents the difference, between the F and C wavelengths, of the power. Most optical glasses have Abbe values between 25 and 70. As is well known, the power of a diffractive element is proportional to the wavelength, and therefore, the equivalent quantity for a diffractive element is:

$$v_{diff} = \frac{(\lambda_d)}{(\lambda_F - \lambda_C)} = -3.45 \tag{2}$$

Note that there is no choice of Abbe number for a diffractive element: its value is chosen once the wavelengths of the design are chosen. Furthermore, regardless of the spectral band, all diffractives in a given optical system have exactly the same Abbe value. Thus, the problem of color correction for an all-diffractive system is the same as that of designing a one-glass achromat, except that the individual elements are more dispersive by about a factor of 10. (The difference in the sign of the Abbe number is of little importance for this discussion.) Therefore, the solution to the one-glass achromat problem may also be applied to the all-diffractive problem.

Next, we consider why a two-element, one-glass Schuppmann system has any secondary color at all. After all, if the system uses only a single glass type and meets the condition for zero primary color at one wavelength, should it not be a solution at all wavelengths? More specifically, following Kingslake [20], one may derive the following expression for the longitudinal color of a system of thin lenses:

$$\Delta_{FC}(\ell') = -\frac{1}{u'^2} \sum_i \frac{\phi_i y_i^2}{v_i} \tag{3}$$

where $\Delta_{FC}(\ell')$ is the F-C variation in the image distance, u' is the marginal ray angle in image space, the ϕ_i are the powers, the y_i are the marginal ray heights, and the v_i are the Abbe values of the various elements. If the elements are all made from the same glass, or if they are all diffractive, then, the v_i all have the same value and may be factored out of the sum, and the longitudinal color vanishes if the remaining sum vanishes, i.e., if:

$$\sum_i \phi_i y_i^2 = 0. \tag{4}$$

Similarly, the expression for the secondary axial color is:

$$\Delta_{dC}(\ell') = -\frac{1}{u'^2} \sum_i \frac{\phi_i P_i y_i^2}{v_i} \tag{5}$$

where the P_i are the 'partial dispersion' values of the individual glasses, defined as:

$$P = \frac{(n_d - n_C)}{(n_F - n_C)}. \tag{6}$$

Here, we pause for a moment to point out that for most available optical glasses, the value of P is correlated to the value of v such that a plot of P vs. v shows an approximately linear relationship between P and v. This relationship is known as the 'normal glass line', and it is easily shown that any achromat made from glasses along the normal glass line will have a secondary color equal to about 1/2200 of its focal length.

For a diffractive element operating in the visible, we can define an equivalent P number as:

$$P_{diff} = \frac{(\lambda_d - \lambda_C)}{(\lambda_F - \lambda_C)} = 0.421. \tag{7}$$

In Eq. (5), the P_i are all the same for a system comprising only one glass type or comprising only diffractive elements and may be factored out of the sum, along with the v_i. In that case, the sum that remains is identical to Eq. (4), and it appears that if Eq. (4) is met, then, not only is the primary color zero, but the secondary color must be identically zero as well. This is not the case, as a simple ray trace shows. Figure 1 shows an example of an all-diffractive Schuppmann system, comprising two diffractive elements of focal lengths 100 and -25 mm, separated by 150 mm.

Figure 1 A diffractive Schuppmann system.

The focal length of the combination is 33.333 mm, and the back focal distance is $\ell' = -16.667$ mm for the d wavelength. In the ray trace, both diffractive elements were modeled as the holograms formed by the interference of waves propagating from two point sources.

Figure 2 compares the spectral variation in the focus distance of the Schuppmann system with that of a 33.333-mm focal length holographic singlet.

As expected, the Schuppmann system has far less chromatic aberration than the holographic singlet and is corrected for 'primary' color in that the focus error has zero derivative at the d wavelength. However, it is evident that the system suffers a large amount of secondary color, in spite of the fact that Eq. (4) is exactly satisfied, and therefore Eqs. (3) and (5) predict that both primary and secondary color must be exactly zero. The question on why Eq. (5) is inaccurate is central to the source of induced aberrations.

The answer to the puzzle is the fact that both Eqs. (4) and (5) rely on the value of y, the marginal ray height, without regard to the wavelength. In other words, the equations assume that the y values are the same for all 3 wavelengths, when, in fact, the blue, green, and red rays begin to diverge from one another starting at the first element. Because of the long propagation distance to the second element, the three colors are significantly separated from each other at the second element; this is something not taken into account by the equations. (We obtained good achromatization in a narrow spectral band surrounding the d wavelength because we used the ray heights at the d line to solve the equations.)

From the above, three important conclusions can be reached. The first is that some correction to the equations is required if they are to be applied to systems containing large airspaces in which the chromatic aberration is uncorrected.
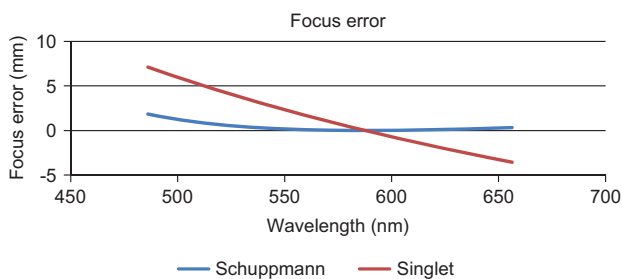
The second conclusion is that the secondary color of this system can be eliminated if the rays for the different colors can be somehow made coincident at the second diffractive element. (We will demonstrate this in the following paragraphs.)

The third conclusion, important but often overlooked, is that large, chromatically uncorrected airspaces can be used to 'induce' secondary color and, if done judiciously, can be used to correct the intrinsic secondary color of the system. This idea was described in detail by McCarthy [21] and later by Wynne [22, 23]. The idea has been used and reviewed by several other authors [24–28].

Returning to the Schuppmann system (and as Schuppmann did in some of his designs), we now place a third (in our case, diffractive) element at the internal focus and adjust its power so that the red and blue rays that begin to diverge from each other at the first element are brought together again at the last element. (This is can loosely be thought of as 'imaging the front element onto the rear element'; however, the two rays that must be brought together are of different wavelengths, so in this instance, the power of the required diffractive element was adjusted slightly so that the red and blue wavelengths are coincident at the last element, with the green wavelength being separated slightly.) Importantly, the diffractive element at the internal image does not introduce axial color of its own, and bringing the red and blue wavelengths together again at the last element restores the accuracy of Eq. (5), so the secondary color is indeed corrected. Figure 3 compares the longitudinal focus shifts for the Schuppmann with and without the field lens. (Note that the vertical scale of the plot has been reduced by a factor of 5 from that of Figure 2.)

Adding the field lens to the Schuppmann system dramatically reduces the residual color by (nearly) recombining the three colors at the last diffractive element, thereby,

Figure 2 Spectral variation in focus for a singlet diffractive element and a Schuppmann system.
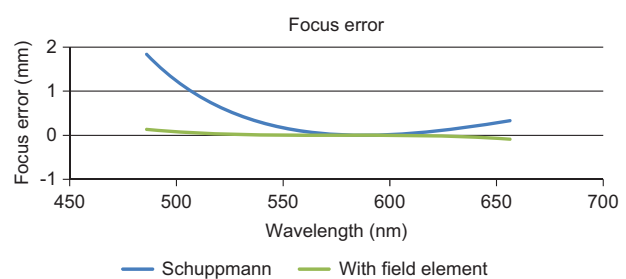
Figure 3 Spectral variation in focus for a two-element Schuppmann system and a Schuppmann with a field element.

restoring the accuracy of Eq. (5). It can be seen that the quadratic dependence of the focal position with the wavelength has been eliminated, with a very small third-order dependence remaining. Offner [29] showed that if the field lens is perfectly achromatic, then all orders of longitudinal color are eliminated. Historically, it is interesting to note that the idea of using a field lens for this purpose originated with Schuppmann, himself, in 1899. The idea of placing a refractive (and achromatic) field lens at the internal image pair of diffractive elements forming a Schuppmann configuration was patented by Hufnagel in 1985 [30]. Direct ray tracing of the all-diffractive Schuppmann shows that, although the secondary axial color is corrected, the secondary lateral color remains. Buralli and Rogers [31] show this to be fundamental to an all-diffractive triplet system. Not surprisingly, the secondary lateral color vanishes if the field lens is perfectly achromatic.

The important thing to be learned from the Schuppmann example is that it is possible to 'induce' the secondary color in an optical system by allowing the colors to drift from each other during propagation through the system.

3 Axial color of separated elements

As a means of exploring the importance of induced chromatic aberrations in refractive designs, we next consider the strength of the induced color aberrations for a pair of separated elements. For this purpose, it is mathematically convenient to depart from the traditional definitions and define 'primary color' as being the first derivative with respect to wavelength and 'secondary color' as being the second derivative with respect to wavelength. Although these are not numerically the same as the traditional definitions, they are not much different in overall meaning, and they enable color aberrations to be examined with simple differentiation.

The power, Φ, of an air-spaced pair of thin elements is:

$$\Phi = \phi_1 + \phi_2 - t\phi_1\phi_2 \tag{8}$$

where ϕ_1 and ϕ_2 are the powers of the two elements, and t is their separation. The back focal distance of the system is given by:

$$\ell' = \frac{1 - t\phi_1}{\Phi}. \tag{9}$$

For the 'primary color', we consider the first derivative of the back focal distance, which is:

$$\frac{\partial \ell'}{\partial \lambda} = \left(\frac{1}{\Phi}\right)\left(-t\frac{\partial \phi_1}{\partial \lambda}\right) - \left(\frac{1}{\Phi^2}\right)(1 - t\phi_1)\frac{\partial \Phi}{\partial \lambda}. \tag{10}$$

It is easily shown that if all the elements are individually achromatic (have zero first derivatives of their powers), then, the primary color as expressed in Eq. (10) is zero. We are interested in the secondary color, so we differentiate Eq. (10) to yield, after considerable manipulation:

$$\frac{\partial^2 \ell'}{\partial \lambda^2} = \frac{-1}{\Phi^2}\left[\frac{\partial^2 \phi_1}{\partial \lambda^2} + \frac{\partial^2 \phi_2}{\partial \lambda^2}\right] + \frac{2}{\Phi^3}\left[\frac{\partial \phi_1}{\partial \lambda} + \frac{\partial \phi_2}{\partial \lambda}\right]^2 - \frac{2t\phi_2}{\Phi^3}\left(\frac{\partial \phi_1}{\partial \lambda}\right)^2$$
$$- \frac{4t\phi_1}{\Phi^3}\left(\frac{\partial \phi_1}{\partial \lambda}\frac{\partial \phi_2}{\partial \lambda}\right) + \frac{t\phi_1\left(6 - 6t\phi_1 + 2t^2\phi_1^2\right)}{\Phi^3}\left(\frac{\partial \phi_2}{\partial \lambda}\right)^2 \tag{11}$$
$$+ \frac{t\phi_1\left(2 - t\phi_1\right)}{\Phi^2}\left(\frac{\partial^2 \phi_2}{\partial \lambda^2}\right)$$

In this expression, the first two terms are independent of t and represent the secondary color intrinsic to the elements themselves. The next three terms represent the secondary color induced by the airspace if the individual elements suffer primary color, i.e., are not achromatized. The last term represents the secondary color induced if the second element suffers an intrinsic secondary color. Thus, we see that if there is a nonzero separation, a secondary color will be induced if the two elements suffer either a primary or secondary color.

We next simplify the problem and ask how much secondary color would be present if every element was made an achromat. In this case, the first derivatives of the powers are zero, and Eq. (11) simplifies to:

$$\frac{\partial^2 \ell'}{\partial \lambda^2}\bigg|_{All-Achr} = \frac{-1}{\Phi^2}\left[\frac{\partial^2 \phi_1}{\partial \lambda^2} + \frac{\partial^2 \phi_2}{\partial \lambda^2}\right] + \frac{t\phi_1\left(2 - t\phi_1\right)}{\Phi^2}\left(\frac{\partial^2 \phi_2}{\partial \lambda^2}\right). \tag{12}$$

Here, the first term represents the intrinsic contributions from the two elements, and the last term (dependent on t) represents the induced contributions.

The induced terms are zero if t=0, as expected. If the separation t is equal to the focal length of the first element (so the second element is located at the focal point of the front element), then $t\phi_1$=1, and the terms dependent on ϕ_2 add to zero, and only the first element contributes. This is expected in the case where an element is located at an image.

The interesting cases are those in which the separation is a substantial fraction of the focal length, but not equal to the focal length, and we now examine two such cases, a Petzval design and a telephoto design.

As a first example, suppose the second element has the same power of the first element and is located halfway to the image formed by the first element; this pair of element forms a Petzval system. We will also assume that the first and second elements are achromats, with a zero primary color and a nonzero secondary color. Starting with Eq. (12) and substituting $t\phi_1=0.5$, we obtain:

$$\frac{\partial^2 \ell'}{\partial \lambda^2}_{Petzval}=\frac{1}{\Phi^2}\left(-\frac{\partial^2 \phi_1}{\partial \lambda^2}-0.25\frac{\partial^2 \phi_2}{\partial \lambda^2}\right). \qquad (13)$$

Assuming that the second element is made of the same materials as the front element, then, as it has the same power of the first, it also has the same secondary color, and we can simplify to it:

$$\frac{\partial^2 \ell'}{\partial \lambda^2}_{Petzval}=\frac{-1.25}{\Phi^2}\frac{\partial^2 \phi_1}{\partial \lambda^2}. \qquad (14)$$

Returning to Eq. (8) and substituting the known values of t and ϕ_2 relative to ϕ_1, we can see that, in this case, the power of the Petzval system is 1.5 times stronger than the front element; in other words, the front element must have 2/3 the power of the overall system. Substituting this into Eq. (14), we obtain:

$$\frac{\partial^2 \ell'}{\partial \lambda^2}_{Petzval}=\left(\frac{5}{6}\right)\frac{-1}{\Phi^2}\left[\frac{\partial^2 \Phi}{\partial \lambda^2}\right]. \qquad (15)$$

For comparison purposes, we now return to Eq. (11) and set t and ϕ_2 to zero and also set the first derivative of ϕ_1 to zero to obtain the result for a single achromat:

$$\frac{\partial^2 \ell'}{\partial \lambda^2}_{Single\ Achromat}=\frac{-1}{\Phi^2}\left[\frac{\partial^2 \Phi}{\partial \lambda^2}\right]. \qquad (16)$$

Comparing Eqs. (15) and (16), we see that separating the elements into a modest Petzval configuration (without resorting to any changes in lens materials) has reduced the secondary color to 5/6 (83%) of the value for a single achromat.

As a second example, consider the case of a telephoto, with the second element having -2/3 the power of the first element and being located halfway to the image formed by the first element. Again, we assume that the two elements are achromats.

We begin again at Eq. (12), and because the second element is halfway to the image, Eq. (13) once again holds. Assuming the second element is made of the same materials as the front element, then, as it has -2/3 the power of the first, it has -2/3 the secondary color. Substituting this into Eq. (13) and simplifying yields:

$$\frac{\partial^2 \ell'}{\partial \lambda^2}_{Telephoto}=\left(\frac{5}{6}\right)\frac{-1}{\Phi^2}\left(\frac{\partial^2 \phi_1}{\partial \lambda^2}\right). \qquad (17)$$

In this telephoto case, with the parameters chosen, the overall system power is 2/3 that of the first element. Therefore, the first element needs to have 1.5 times the power of the system, and substituting this into Eq. (15) gives:

$$\frac{\partial^2 \ell'}{\partial \lambda^2}_{Telephoto}=(1.25)\frac{-1}{\Phi^2}\left(\frac{\partial^2 \Phi}{\partial \lambda^2}\right). \qquad (18)$$

Comparing to Eq. (16), we see that in the telephoto case, separating the achromats while leaving their composition unchanged has *increased* the secondary color by 25% relative to a single achromat. However, in the telephoto case, the second element is of the opposite sign from the first and, therefore, contributes a secondary color of the opposite sign. In such a case, the total secondary color can be reduced designing the second achromat to have an intentionally large amount of secondary color. Up until this point, we have used the same materials for all achromats, under the assumption that we will select the best materials that have acceptable cost, thermal expansion, and transmission properties. However, for the negative achromat, it is desirable to depart from this and design an achromat with a large (negative) amount of secondary color. This is easily achieved using two glasses whose v and P values are both widely separated. For instance, it is easily verified that a doublet made from NLAK10 and NSF11 has 60% more secondary color than one made of NPSK53A and F2. Therefore, we will assume that the second achromat introduces, per unit power, 1.6 times as much secondary color as the first achromat. This increases the second (ϕ_2) term in Eq. (13) by a factor of 1.6 and after simplification yields:

$$\frac{\partial^2 \ell'}{\partial \lambda^2}=\frac{0.9}{\Phi^2}\left(-\frac{\partial^2 \Phi}{\partial \lambda^2}\right). \qquad (19)$$

Thus, in this telephoto example, we were able to reduce the secondary color by 10% compared to a single achromat made of the same materials as the first achromat of the telephoto. This did not occur naturally and required that we intentionally choose materials that yield a large amount of secondary color for the second achromat. It is generally true that it is harder to reduce the secondary color of telephoto (and also reverse telephoto) systems than for Petzval systems. However, the example has shown that it is sometimes advantageous to intentionally increase the amount of color in one or more elements.

4 Lateral color of separated elements

Having examined the case of the secondary axial color, some remarks concerning the secondary *lateral* color are in order. Assuming the longitudinal color is well-corrected, the lateral color is equivalent to the chromatic difference of magnification or, for an object at infinity, the chromatic difference of the focal length. The latter is related in a simple way to the chromatic difference of the power, and the equations for the first and second derivatives of the power can be derived in a manner entirely analogous to the above treatment of the focal shift. The derivation is simpler for the lateral color than for the longitudinal color, and we will simply give the result:

$$\frac{\partial^2 \Phi}{\partial \lambda^2} = \left(\frac{\partial^2 \phi_1}{\partial \lambda^2} + \frac{\partial^2 \phi_2}{\partial \lambda^2} - t\phi_1 \frac{\partial^2 \phi_2}{\partial \lambda^2} - t\phi_2 \frac{\partial^2 \phi_1}{\partial \lambda^2} \right). \tag{20}$$

Here again, we recognize two intrinsic terms and two induced terms, and the induced terms vanish if $t=0$. If $t\phi_1=1$, the contribution from the second element vanishes, and we are left with:

$$\frac{\partial^2 \Phi}{\partial \lambda^2} = \left(\frac{\partial^2 \phi_1}{\partial \lambda^2} - t\phi_2 \frac{\partial^2 \phi_1}{\partial \lambda^2} \right). \tag{21}$$

Interestingly, the contribution of the second element to the secondary lateral color (more precisely, to the secondary spectral variation of the power) does not vanish if the second element is placed at the image formed by the first element. This is because of the slight focal shift between the green and blue/red components, which allows the second element to alter (slightly) the departing ray angles of the blue/red rays.

5 Simultaneous correction of axial and lateral color: a graphical approach

When considering the lateral color, it is important to note that no system of two thin elements can be corrected simultaneously for both the secondary longitudinal and secondary lateral color, unless the individual elements are, themselves, corrected for secondary color. The reason is that the longitudinal color correction of the system requires that the rays of all the colors focus at the same point, whereas the secondary color of the front element causes the green rays to split from the blue/red rays and,

therefore, strike the second element at a different height. This implies that the green rays approach the final image at a different numerical aperture than the blue/red rays, so the chromatic difference of magnification cannot be zero. Using this line of logic, it is easy to see that the minimum number of separated elements required for the simultaneous correction of the secondary lateral and secondary longitudinal color (without requiring the individual elements to be corrected) is three, as Figure 4 demonstrates conceptually.

In the figure, the rays of all the colors enter the system together and are shown in black. After the first element, the green light separates from the red and blue rays, which are shown together in magenta. In order to be free of both the longitudinal and lateral color, all the rays must recombine at the last element and propagate (as shown again in black) toward the image at the same numerical aperture. To achieve this, the middle element must, therefore, refract the green rays more strongly from the blue/red rays, so that they recombine at the third element.

A little thought tells us that the positive-negative-positive (PNP) configuration shown in Figure 4 is an excellent candidate for a system that might be corrected for both the longitudinal and lateral secondary color, with minimum use of special glasses. The front element refracts the green light more strongly than the blue/red, as would be expected for an achromat with a positive power. Similarly, if we imagine the rays to be traced backward from the image, through the rear element toward the central element, we see that the positive rear element also refracts the green light more strongly than the blue/red, and this is consistent with what we expect from an achromat. Finally, we note that the middle element is negative, and it also refracts the green light more strongly than the blue/red pair, as would be expected. Thus, we see that at least the signs of the required secondary color contributions are consistent with the behavior of ordinary glasses. One might expect that the negative element might need to contribute more secondary color per unit power than the outer two elements, as the green light is at a higher angle than the blue/red on both sides of the element. As we
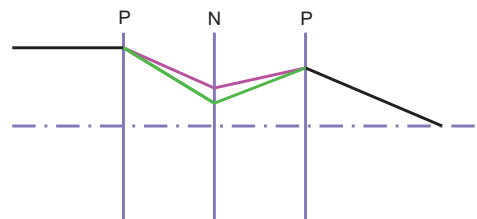
Figure 4 Conceptual example of a three-element system corrected for both longitudinal and lateral color.
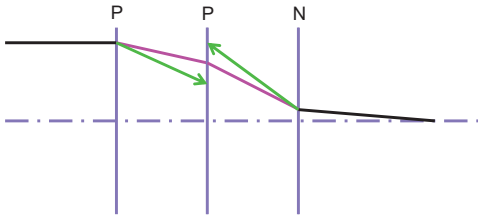
Figure 5 Conceptual drawing of a system that cannot be corrected for both secondary axial and secondary lateral color.

pointed out earlier, it is generally easier to design achromats with large amounts of secondary color than small amounts of secondary color, so this appears to be a good candidate system. (We will return to this system later.)

Figure 5 shows an example of a configuration of three achromats that clearly *cannot* be easily corrected for secondary color.

Tracing the rays from the object and image toward the middle element, we see that if the green rays behave as expected at the outer two elements, they cannot possibly connect at the central element. Evidently, the only way for this system to be corrected for both the secondary longitudinal and secondary lateral color is for at least one of the outer elements to be overcorrected for the secondary color; this is not realistic in most spectral bands.

The conceptual drawing of the type shown in Figures 4 and 5 is an excellent way of determining whether a configuration can likely be corrected for the secondary color. With three elements and two possible signs of P and N, there are eight possible configurations, seven of which contain at least one P element. By sketching these seven configurations in the manner shown, one can see very quickly that only the PNP and the NPN configurations show any promise for the secondary correction of both color aberrations. In both cases, we expect that the middle element would need to contribute a larger-than-usual amount of secondary color.

6 Design example: a three-doublet system

We next consider an actual design example, in which the elements are optimized to maximize performance. Here, it is important to realize that in any real design, chromatic aberration correction is not the only consideration. Realistically, small amounts of longitudinal color are often left in the system to balance the chromatic variation of spherical aberration (spherochromatism), and the lateral color is often left in the system to balance against the chromatic

variation of coma. This is not to say that a study of chromatic aberration correction is worthless. As Shafer has pointed out [32], it is important to understand how to correct individual aberrations, even if the target values used in the final design problem are not zero.

For our design example, we will use a focal length of 500 mm. An ordinary achromat of this focal length would have a longitudinal color of about 500/2200=227 μm. To ensure that the chromatic aberrations are not obscured by larger, 'monochromatic' aberrations, we will design the system at a relatively slow F-number of F/10, and we will optimize over a relatively modest full field angle of 10°. The diffraction-limited depth of focus of an F/10 system is about 100 μm, so the 227 μm of secondary color of an ordinary achromat would be significant, even if we ignore the fact that an ordinary achromat could not cover a 10° full field.

The design configuration we will use as a starting point for optimization is the three-doublet PNP configuration that was suggested as promising by Figure 4. We constrain the focal length to 500 mm, and we, at first, constrain the three doublets to be individually achromatic to obtain a 'baseline' design with minimal induced aberrations.

We begin by using the global optimization feature of CODE V® [33], allowing the glasses to vary, but requiring them to lie on the normal glass line and requiring the primary axial color of each achromat to be zero. We also constrain the length of the system to be <700 mm. The best design resulting from global optimizations is essentially a pair of achromats with (what appears to be) a field flattener, as shown in Figure 6. In this design, all three doublets have positive power; the third doublet is correcting the natural astigmatism introduced by the first two doublets.

As a second step, we converted to the nearest real glass types and use CODE V's Glass Expert feature to search for replacement glasses that improve the performance from the all-normal-glass starting point. For this step, we still required that each doublet be individually achromatic, but we allowed the use of glasses that departed modestly
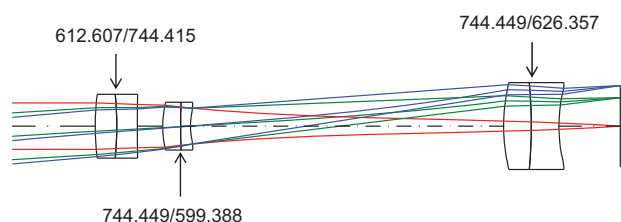
Figure 6 System of three achromats, found by global optimization with fictitious glasses.

from the normal glass line. As we want to demonstrate what can be accomplished without resorting to the use of special glasses, we selected glasses from a very conservative set of glasses, excluding from consideration the following glass types:

– all FK and NFK glasses,
– all KZFS and NKZFS glasses,
– all lead-containing glasses.

We also imposed a requirement that the coefficients of linear expansion of the glasses that are to be cemented together match reasonably well; specifically, we required the radial shear of the two elements, calculated at the edge of the clear aperture without regard to cement properties, be <0.1 μm per degree Celsius.

The solution found is shown in Figure 7, and Figure 8 shows the longitudinal aberrations of the system.

From Figure 8, we can see that the primary axial color is approximately corrected, i.e., the red and blue focal planes coincide, but a substantial amount of secondary color remains. The secondary color is 231 μm, as the ratio of the focal length is 1:2164, which is about what

Figure 7 System of three achromats, after selecting optimal glasses from a restricted list.

Figure 8 Longitudinal aberrations of the system in Figure 7.

we would expect from an ordinary achromat. We can see from Figure 8 that the spherical aberration is small, and there is almost no variation of spherical with wavelength. Although we are primarily interested in the on-axis aberrations for this exercise, we will comment that this system has little lateral color and is corrected to have a flat tangential field. The polychromatic RMS wavefront variance for this system ranges from 0.0725 λ on axis to 0.0772 λ at the edge of the field. According to Marechal's criterion [34], we can say this system is very close to 'diffraction limited' over the field.

Next, we drop the requirement that the three doublets be individually achromatic and repeat the global optimization procedure, beginning with fictitious glasses, constrained to lie on the normal glass line. After that, we again convert the glass types from fictitious to real glasses (selecting from the same glass list as before) and use Glass Expert (with the same restriction on CTE mismatch) to obtain the best glasses for this new configuration. The best configuration found for the case in which the doublets are not required to be individually color corrected is the NPN configuration shown in Figure 9.

It is interesting to note that the two outer doublets contain NPSK53A, a glass type well-known to be useful for reducing the secondary color in achromats. On the other hand, the inner doublet is made of two flints and introduces more than 5 mm of axial color that is corrected by an axial color of the opposite sign in the two outer doublets, which are, in this case, far from achromatic. As Figure 10 shows, the performance of the overall system is far superior to that of an achromat. *Note that the scale of aberrations in Figure 10 has been reduced by a factor of 10 from that of Figure 8*.

The paraxial secondary color is 22 μm, down from 231 for the three-achromat design. (As a fraction of the focal length, 22 μm represents 1 part in 22 700.) At this aberration scale, the variation of spherical aberration with wavelength is plainly visible in the plot; however, the total variation of the focal position, considering both wavelength and aperture, is 35 μm, well below the 100-μm depth of focus of this F/10 system. In this design, the
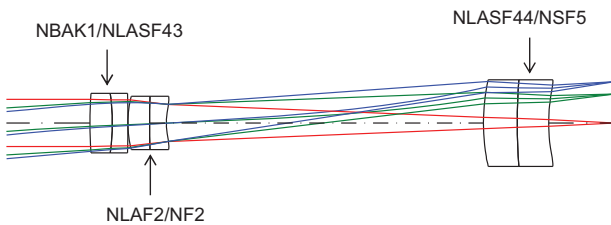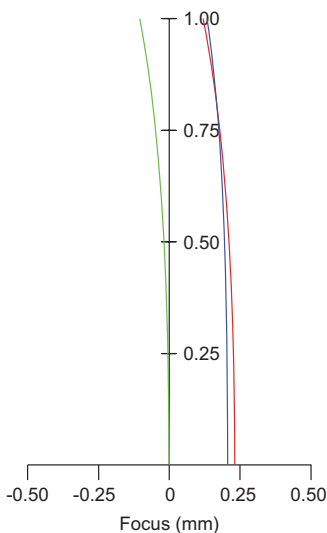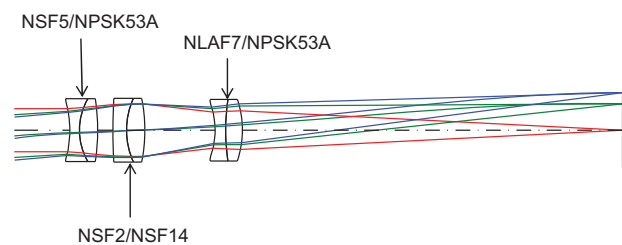
Figure 9 NPN system with real glass types.
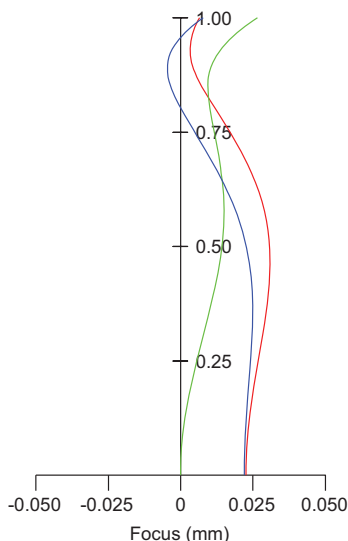
Figure 10 Longitudinal aberrations of the system in Figure 9.

combination of the individually uncorrected doublets and their separations induces an amount of secondary color that offsets 90% of the natural secondary color that one would expect from a 500-mm focal length achromat. This degree of correction is achieved without the use of any special glass types. As an added performance bonus, the three-doublet system is able to cover a much wider field than an achromat would be able to cover. The RMS wavefront values for this system range from 0.007 λ on axis to 0.026 λ at the edge of the field.

7 Aberration balancing and tolerance sensitivity

One drawback to the use of induced aberrations to correct a system is that when separated elements introduce large, counterbalancing amounts of aberrations, the system is more sensitive to misalignments. From the standpoint of sensitivities, it is generally a better idea to correct the aberrations in the elements, themselves, than to allow one element to balance the aberrations of another. However, it is often simply not possible to achieve the desired degree of intrinsic color correction within the constraints imposed by cost, thermal expansion, and transmission considerations. To examine this effect, we carried out a tolerance analysis to compare the anticipated RMS wavefront error values of the three-achromat (Figure 7) system and the three-doublet (Figure 9) system in their 'as-built' states.

For any comparison of the as-built performance, the choice of tolerance level is an important one. If the tolerances are chosen so loosely that the tolerance-induced aberrations are several times larger than the nominal performance, then the tolerance-induced effects will clearly dominate the performance, and any extra care taken to correct or even improve the secondary color is wasted (or worse, if the secondary color correction increases the sensitivity of the system). Therefore, for this comparative study, we first select a set of tolerances and compensators that allows a modest (approximately 30%) worsening of the RMS wavefront for the three-achromat baseline system, and then, we apply those same tolerances and compensators to the system that employs induced color aberrations.

We begin with the three-achromat system of Figure 7 and – as an initial guess – assign tolerances that can be considered to correspond roughly to a set of 'drop-in' tolerances, using 'unselected' glass tolerances. These tolerances are:

– radius errors: ±0.1% of the radius value,
– surface irregularity: 1 fringe at 632.8 nm,
– thickness errors: ±25 μm,
– air space errors: ±25 μm,
– refractive index errors: ±0.001,
– Abbe values ±0.8%,
– element wedge: 10 μm of total indicated runout (TIR),
– doublet wedge: 10 μm of total indicated runout (TIR),
– doublet tilt: 10 μm of total indicated runout (TIR),
– doublet decentration: 50 μm (comprising 25 μm ID error on the tube and 25 μm OD error on the lens),
– compensation of focus only.

For this initial analysis, we assume that the only post-assembly adjustment to the system will be to adjust the spacing to the detector, for optimal focus averaged over the image plane. With this set of tolerances, using only refocus as a compensator, the RMS wavefront approximately triples from 0.072 λ to 0.206 λ on the axis, and from 0.077 λ to 0.2234 λ at the edge of the field. Thus, we immediately see that this 'drop-in' set of tolerances is far from what is necessary for a realistic comparison.

Not surprisingly for a slow, long-focal-length system, the sensitivities are dominated by tolerances on the Abbe value and irregularity, with tolerances on the decenter and wedge being also important. To improve the performance, we, therefore, tighten the index and Abbe tolerances and implement a respace between the elements that is to be carried out after the indices, Abbe values, and radii are known. We also designate the middle doublet to have an intentional decentration to compensate for the

decentration and wedge tolerances of the other elements. The tightened set of tolerances is as follows:

- radius errors: ±0.05% of the radius value,
- surface irregularity: 0.3 fringe at 632.8 nm,
- thickness errors: ±25 μm,
- refractive index errors: ±0.00003 (=Schott 'Step 1'),
- Abbe values ±0.2% (=Schott 'Step 1'),
- element wedge: 10 μm of total indicated runout (TIR),
- doublet wedge: 10 μm of total indicated runout (TIR),
- doublet tilt: 10 μm of total indicated runout (TIR),
- doublet decentration: 50 μm (comprising 25 μm ID error on the tube and 25 μm OD error on the lens),
- airspaces adjusted to compensate for errors in radius, index, and Abbe,
- decenter of the second doublet used as an at-assembly compensator,
- compensation of focus.

With this tightened set of tolerances and using the compensators listed, we carried out a 1000-case Monte Carlo based on the wavefront differentials for the individual tolerances, for both systems. The results, for both the three-achromat (Figure 7) system and the three-doublet (Figure 9) system are summarized with the cumulative probability curves shown in Figure 11.

In the figure, the horizontal axis is the RMS wavefront variance with values increasing (worse performance) toward the right, and the vertical axis is the cumulative probability or attaining a given RMS value or better. For instance, the green line shows that the three-achromat system, on the axis, is expected to attain an RMS wavefront variance of 0.08 λ, or better, with a probability of about 40% (or in 40% of the cases, if a large number of systems is assembled.) For each curve, the low-probability extreme (the intercept with the horizontal axis) represents

the nominal (pretolerance) performance, and the high-probability extreme represents the estimate of performance that will be reached even approaching the 'worst case scenario'. The horizontal intercepts of the blue and red curves lie to the left (better than) of the green and purple curves, reflecting the fact that the nominal performance of the three-doublet system is better than that of the three-achromat system.

The fact that the curves for the three-achromat system rise more steeply is an indication that the three-achromat system is (as expected) less sensitive than the three-doublet system (i.e., there is a smaller difference than the best case and the worst case). In this particular case, the nominal performance of the three-doublet system is so much better than that of the three-achromat system and that the three-doublet curves lie to the left of the three-achromat curves except at the extreme worst-case limit, where the performance values are very similar. It can be seen, for instance, that the on-axis RMS value for the three-doublet case will be better than 0.07 λ in about 86% of the cases, whereas the three-achromat system will achieve an on-axis RMS 0.07 λ in only about 10% of the cases.

It is clear that, in this case (with the relatively tight set of tolerances chosen), the three-doublet system with induced aberrations outperforms the three-achromat system. In other cases (different designs or the same designs with a different set of tolerances), the reverse might be true, so it is important to keep the as-built performance in mind when intentionally adding induced aberrations to a design.

8 Conclusions

Substantial amounts of secondary color can be induced in the spaces between optical elements. This is particularly true when the elements, themselves, are not individually corrected for primary color, but the effect can be significant even in the airspaces between the elements that are corrected for primary color. Certain configurations lend themselves more readily than others to the reduction of the secondary color, and the method depicted in Figures 4 and 5 can be used to explore which configurations are the most promising. Global optimization is another good way to find design configurations with low residual color. Global optimization is particularly useful when other effects such as the chromatic variation of aberrations are significant factors in a design.

Although the design example shown above was kept slow for the sake of clarity, induced aberrations are no less
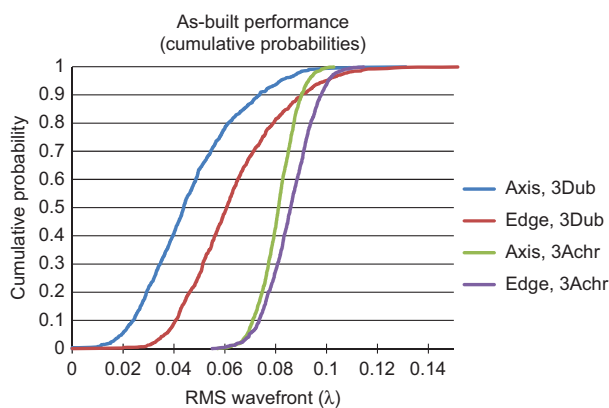
Figure 11 Cumulative probabilities for the three-achromat and three-doublet designs.

important when the system is faster or covers a wider field. All of the aberrations (including both spherical aberration and spherochromatism) have induced components, and while the mix of aberrations may be more confusing at faster numerical apertures, the importance of the induced aberration components is not reduced.

Induced secondary color can have a deleterious effect on an optical system, or if handled carefully, it can allow a better degree of optical correction than would otherwise be the case with the allowed set of glasses. As design tools, induced aberrations must be used judiciously or else the benefit in nominal performance may be overwhelmed by the increased sensitivity of the system.

References

[1] N. v. d. W. Lessing, J. Opt. Soc. Am. 48, 269–271 (1958).
[2] R. Stephens, J. Opt. Soc. Am. 49, 398–399 (1949).
[3] R. Stephens, J. Opt. Soc. Am. 50, 1016–1019 (1960).
[4] M. Herzberger and N. McClure, Appl. Opt. 2, 553–560 (1963).
[5] A. Mikš and J. Vondřich, Optik 28, 321–327 (1968).
[6] N. v. d. W. Lessing, Appl. Opt. 9, 1665–1668 (1970).
[7] M. Shpyakin, Sov. J. Opt. Technol. 45, 81–83 (1978).
[8] R. Mercado and P. Robb, J. Opt. Soc. Am 71, 1639 (1981).
[9] R. Mercado and P. Robb, J. Opt. Soc. Am 72, 1725 (1982).
[10] R. Mercado and P. Robb, J. Opt. Soc. Am 73, 1882 (1983).
[11] R. Mercado, SPIE 554, 217–227 (1985).
[12] P. Robb, SPIE 554, 60–75 (1985).
[13] P. Robb, Appl. Opt. 24, 1864–1877 (1985).
[14] H. Buchdahl, Appl. Opt. 24, 1878–1882 (1985).
[15] A. G. Schott, Mainz, Germany
[16] L. Schuppmann, in Die Mediale-Fernrohre. Eine Neue Konstruktion für Grosse Astronomische Instrumente (B.G. Teubner, Leipzig, 1899).
[17] R. Katyl, Appl. Opt. 11, 1241–1247 (1972).
[18] J. Latta, Appl. Opt. 11, 1686–1696 (1972).
[19] I. Weingärtner and K. Rosenbruch, Optica Acta 29, 519–529 (1982).
[20] R. Kingslake, in Lens Design Fundamentals (Academic Press, New York, 1978), pp. 77–84.
[21] E. L. McCarthy, US Patent 2,698,555 (1955).
[22] C. Wynne, Opt. Comm. 21, 419–424 (1977).
[23] C. Wynne, Optica Acta 25, 627–636 (1978).
[24] R. Stephens, J. Opt. Soc. Am. 47, 1135 (1957).
[25] G. Mozharov, Sov. J. Opt. Technol. 44, 146–148 (1977).
[26] M. Rosete-Aguilar, SPIE 2774, 378–386 (1996).
[27] R. Duplov, Appl. Opt. 45, 5164–5167 (2006).
[28] A. Grammatin and E. Tsyganok, J. Opt. Technol. 79, 202–204 (2012).
[29] A. Offner, Appl. Opt. 8, 1735–1736 (1969).
[30] R. Hufnagel, US Patent 4,550,973 (1985).
[31] D. Buralli and J. Rogers, J. Opt. Soc. Am. A 6, 1863–1868 (1989).
[32] D. Shafer, Proc. SPIE 1354, 608–616 (1991).
[33] CODE V is a registered trademark of Synopsys Inc.
[34] A. Maréchal, Rev. Opt. Theor. Instrum. 26, 257–277 (1947).

John Rogers, PhD, is a Senior Scientist for Imaging Optics at Synopsys. He received his PhD from the Optical Sciences Center at the University of Arizona in 1984, and spent 10 years working as an optical designer and metrologist in the Swiss optical industry, at Kern AG and later at Leica. For 4 years, he taught geometrical optics and optical testing at the University of Rochester. In 1987, he joined Optical Research Associates (now Synopsys) where, working in the Engineering Services group, he has designed a wide variety of optical systems.